



Preliminary Experiments on Accelerator-Driven Subcritical Reactor with Pulsed Neutron Generator in Kyoto University Critical Assembly

Cheol Ho PYEON , Yoshiyuki HIRANO , Tsuyoshi MISAWA , Hironobu UNESAKI , Chihiro ICHIHARA , Tomohiko IWASAKI & Seiji SHIROYA

To cite this article: Cheol Ho PYEON , Yoshiyuki HIRANO , Tsuyoshi MISAWA , Hironobu UNESAKI , Chihiro ICHIHARA , Tomohiko IWASAKI & Seiji SHIROYA (2007) Preliminary Experiments on Accelerator-Driven Subcritical Reactor with Pulsed Neutron Generator in Kyoto University Critical Assembly, Journal of Nuclear Science and Technology, 44:11, 1368-1378, DOI: 10.1080/18811248.2007.9711384

To link to this article: <https://doi.org/10.1080/18811248.2007.9711384>



Published online: 05 Jan 2012.



Submit your article to this journal [↗](#)



Article views: 585



View related articles [↗](#)



Citing articles: 7 View citing articles [↗](#)

ARTICLE

Preliminary Experiments on Accelerator-Driven Subcritical Reactor with Pulsed Neutron Generator in Kyoto University Critical Assembly

Cheol Ho PYEON^{1,*}, Yoshiyuki HIRANO^{2,†}, Tsuyoshi MISAWA¹, Hironobu UNESAKI¹,
Chihiro ICHIHARA¹, Tomohiko IWASAKI³ and Seiji SHIROYA¹

¹*Nuclear Engineering Science Division, Research Reactor Institute, Kyoto University,
Asashiro-nishi, Kumatori-cho, Sennan-gun, Osaka 590-0494, Japan*

²*Department of Fundamental Energy Science, Graduate School of Energy Science, Kyoto University,
Yoshida-honmachi, Sakyo-ku, Kyoto 606-8501, Japan*

³*Department of Quantum Science and Energy Engineering, Graduate School of Engineering,
Tohoku University, Aramaki, Aoba-ku, Sendai 980-8579, Japan*

(Received February 16, 2007 and accepted in revised form July 11, 2007)

A series of preliminary experiments on an accelerator-driven subcritical reactor (ADSR) with 14 MeV neutrons were conducted at Kyoto University Critical Assembly (KUCA) with the prospect of establishing a new neutron source for research. A critical assembly of a solid-moderated and -reflected core was combined with a Cockcroft-Walton-type accelerator. A neutron shield and a beam duct were installed in the reflector region for directing as large a number as possible of the high-energy 14 MeV neutrons generated by deuteron-tritium (D-T) reactions to the fuel region, since the tritium target is located outside the core. And then, neutrons (14 MeV) were injected into a subcritical system through a polyethylene reflector. The objectives of this paper are to investigate the neutron design accuracy of the ADSR with 14 MeV neutrons and to examine experimentally the neutronic properties of the ADSR with 14 MeV neutrons at KUCA. The reaction rate distribution and the neutron spectrum were measured by the foil activation method for investigating the neutronic properties of the ADSR with 14 MeV neutrons. The eigenvalue and fixed-source calculations were executed using a continuous-energy Monte Carlo calculation code MCNP-4C3 with ENDF/B-VI.2 for the subcriticality and the reaction rate distribution, respectively; the unfolding calculation was done using the SAND-II code coupled with JENDL Activation Cross Section File 96 for the neutron spectrum. The values of the calculated subcriticality and the reaction rate distribution were in good agreement with those of the experiments. The results of the experiments and the calculations demonstrated that the installation of the neutron shield and the beam duct was experimentally valid and that the MCNP-4C3 calculations were accurately carried out for analyzing the neutronic properties of the ADSR with 14 MeV neutrons at KUCA.

KEYWORDS: ADSR, KUCA, solid-moderated core, preliminary experiments, neutron shield, beam duct, 14 MeV pulsed neutrons, foil activation method, MCNP, neutronic properties

I. Introduction

The accelerator-driven subcritical reactor (ADSR) has been developed for producing energy and for transmuting minor actinides and long-lived fission products. The ADSR has attracted worldwide attention¹⁻⁶⁾ in recent years because of its superior safety characteristics and potential for burning plutonium and nuclear waste. An outstanding advantage of its use is the anticipated absence of reactivity accidents, provided sufficient subcriticality is ensured.

At the Kyoto University Research Reactor Institute (KURRI), a series of preliminary experiments on the ADSR with 14 MeV neutrons was officially launched at Kyoto University Critical Assembly (KUCA)⁷⁻¹⁵⁾ as a joint-use program among Japanese universities, with prospects of a future plan (Kart & Lab. Project).^{16,17)} The goal of the plan is to establish a next-generation neutron source, as a substitute for the current 5 MW Kyoto University Reactor (KUR) established in 1964, by introducing a synergetic system comprising a research reactor and a particle accelerator. The construction of a new accelerator has been completed and its beam commissioning is currently being conducted. It is expected that high-energy neutrons, generated by the interaction of high-energy proton beams (150 MeV) with heavy metal, could be injected into KUCA and that the ADSR experiments with 150 MeV protons could start in the near

*Corresponding author, E-mail: pyeon@kuca.rii.kyoto-u.ac.jp

†Present address: Department of Earth and Space Science, Graduate School of Science, Osaka University, Yamadaoka, Suita-shi, Osaka 565-0871, Japan

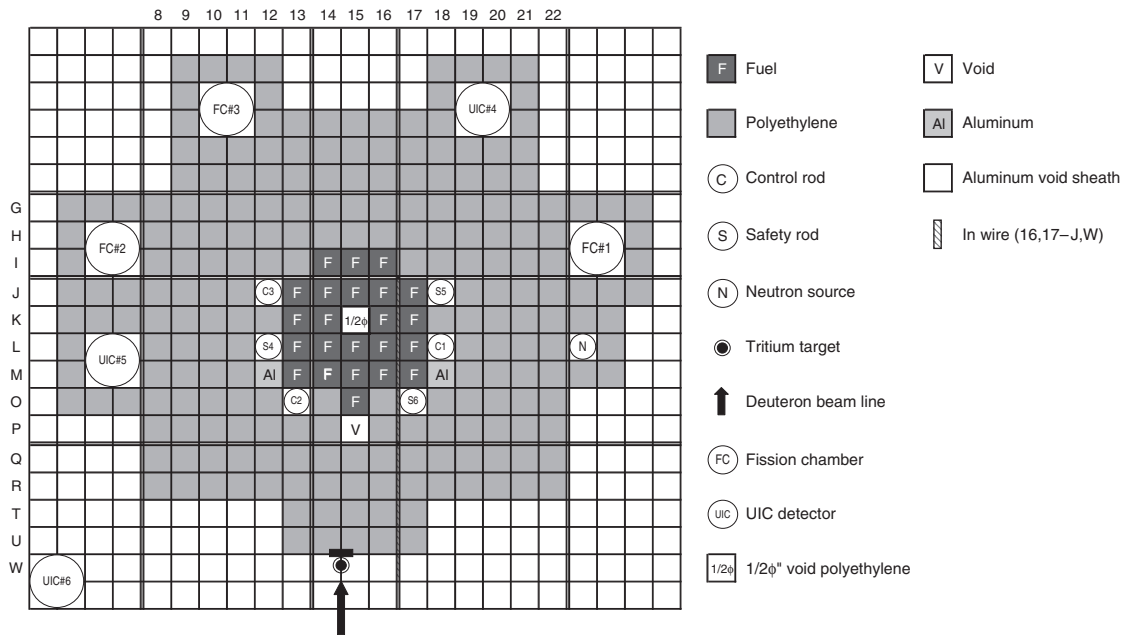


Fig. 1 Top view of configuration of A-core experiments (Reference core: Case 1)

future. The new accelerator is called the Fixed Field Alternating Gradient (FFAG) accelerator of the synchrotron type¹⁸⁻²⁰⁾ developed by the High Energy Accelerator Research Organization (KEK) in Japan. The research and development program of the projected plan includes the fields of accelerators, materials, thermal hydraulics and reactor physics. Among these, the present field of reactor physics is devoted to neutronic studies on the subcritical system of the ADSR with 150 MeV protons, especially that neutronic design analyses are considered essential for research in new neutron sources.

Prior to the ADSR experiments with 150 MeV protons, it is necessary to establish measurement techniques for various neutronic parameters and the method for evaluating neutronic properties of the ADSR with 150 MeV protons. For these purposes, a series of preliminary experiments with 14 MeV neutrons has been carried out using a core and a pulsed neutron generator of KUCA. At KUCA, by combining a critical assembly of a solid-moderated and -reflected type-A core with a Cockcroft-Walton-type accelerator,²¹⁾ 14 MeV pulsed neutrons generated by D-T reactions were injected through a polyethylene reflector into the subcritical system, where highly enriched uranium fuel was loaded together with the polyethylene-moderated reflector.

In these preliminary experiments, subcriticality was varied systematically by inserting control or safety rods, or both, into the critical system. The reaction rate distribution and the neutron spectrum were then measured by the foil activation method. Numerical simulations were executed, with the use of the continuous-energy Monte Carlo calculation code MCNP-4C3²²⁾ with ENDF/B-VI.²³⁾ and JENDL Activation Cross Section File 96.²⁴⁾ In the present study, a neutron shield and a beam duct were installed in the reflector region for directing the high-energy neutrons generated in a tritium target to the fuel region, since the tritium target used by D-T

reactions is located outside the core. A series of these experiments were performed in a slightly subcriticality state of around $k_{eff} = 0.99$. The main objectives of the present experiments are to investigate the accuracy of the neutronic design of the ADSR with 14 MeV neutrons in its present state, to experimentally examine the neutronic properties of the ADSR with 14 MeV neutrons at KUCA through the reaction rate distribution and the neutron spectrum and to establish measurement techniques for neutronic parameters in the subcritical system.

The ADSR preliminary experiments with 14 MeV neutrons at KUCA, including the core configuration and the measurement techniques, are presented in Sec. II the results of experiments and analyses using MCNP-4C3 in Sec. III, and the conclusion of the study in Sec. IV.

II. ADSR Experiments

1. Description of KUCA Facility

KUCA comprises solid-moderated and -reflected type-A and -B cores, and a water-moderated and -reflected type-C core. In the present series of experiments, the solid-moderated and -reflected type-A core was combined with a Cockcroft-Walton-type pulsed neutron generator installed at KUCA.

The A-core (A3/8''P36EU(3)) configuration used for measuring the reaction rate distribution and the neutron spectrum is shown in Fig. 1 (Reference core: Case 1). The A-core was composed of a combination of 23 fuel rods that were loaded on the grid plate. The materials used in the critical assemblies were always in the form of a rectangular parallelepiped, normally 2'' sq. with thickness ranging between 1/16'' and 2''. The upper and lower parts of the fuel region were polyethylene reflector layers of more than 50 cm length, as shown in Fig. 2. The fuel rod, a 93% enriched ura-

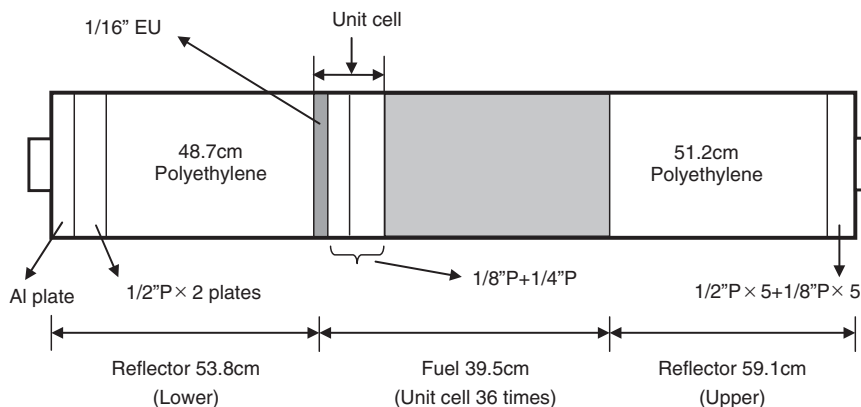


Fig. 2 Side view of configuration of fuel rod of A3/8''P36EU(3) in KUCA A-core (EU: Enriched uranium, Al: Aluminum, P: Polyethylene)

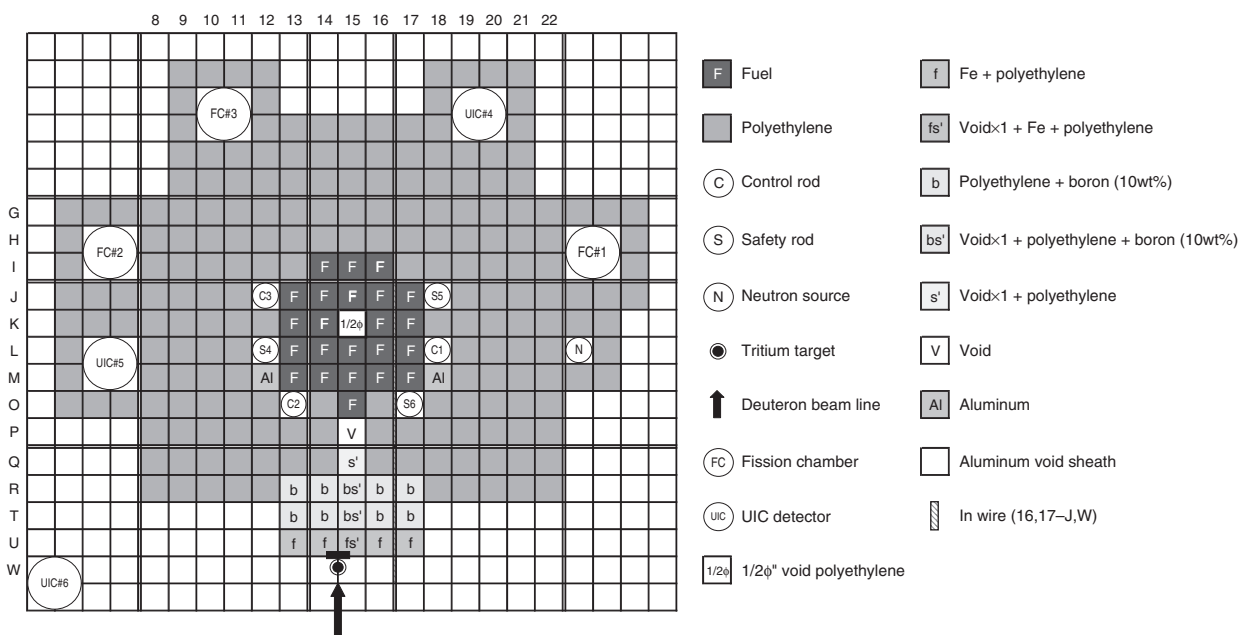


Fig. 3 Top view of configuration of A-core experiments (Neutron shield core with small beam duct: Case 2)

nium-aluminum (U-Al) alloy, consisted of 36 cells of polyethylene plates 1/8'' and 1/4'' thick, and a U-Al plate 1/16'' thick and 2'' sq. The functional height of the core was approximately 40 cm.

The pulsed neutron generator was combined with the A-core, where 14 MeV pulsed neutrons were injected into the subcritical system through the polyethylene reflector. In the experiments, the deuteron beam (accelerated up to 160 keV in beam energy, 0.5 mA in beam current, 10 μs in pulse width and 500 Hz in pulse repetition rate) was led to the tritium target located outside the polyethylene reflector. At the pulsed neutron generator, the beam peak intensity is about 6.5 mA for a pulse width of up to 100 μs, and the repetition rate varies from a few Hz to 30 kHz, providing up to 1×10^8 n/s. The main characteristics of the KUCA pulsed neutron generator are shown in **Table 1**.

2. Installation of Neutron Shield and Beam Duct

The present configuration of the ADSR with 14 MeV

Table 1 Main characteristics of KUCA pulsed neutron generator

Deuteron beam energy (keV)	300 (Maximum)
Beam current (mA)	6.5 (Maximum)
Pulse repetition rate (Hz)	0.1–30,000
Pulse width (μs)	0.3–100
Spot size (mmφ)	25
Duty ratio (%)	1 (Maximum)

neutrons at KUCA is slightly different from that of other ADSR systems, because the tritium target is located outside the core. The tritium target of the pulsed neutron generator was not easily moved to the center of the core, because control and safety rods were, as a couple of the control drive system, fixed in the core. Moreover, a new tritium target would affect neutron multiplication of the core by perturbation of the new target installed in the center of the core. This is because the core size of the fuel region is only

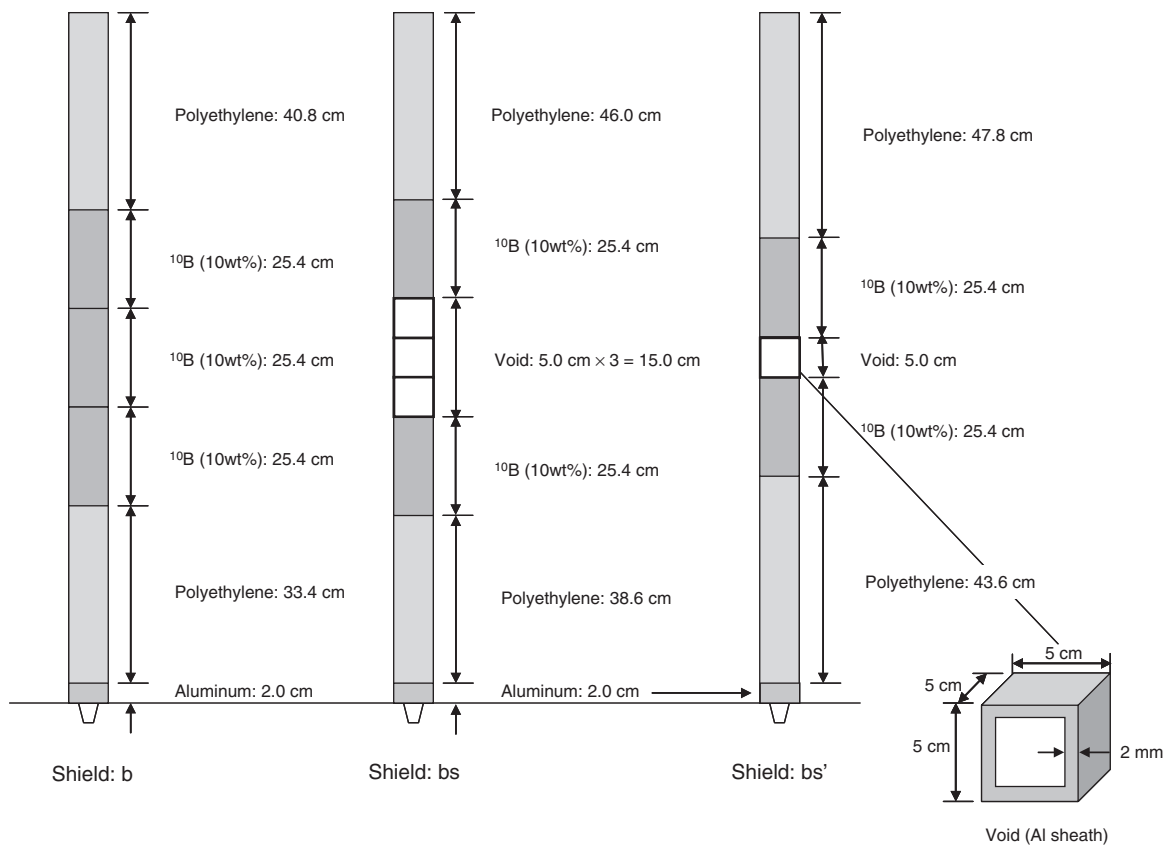
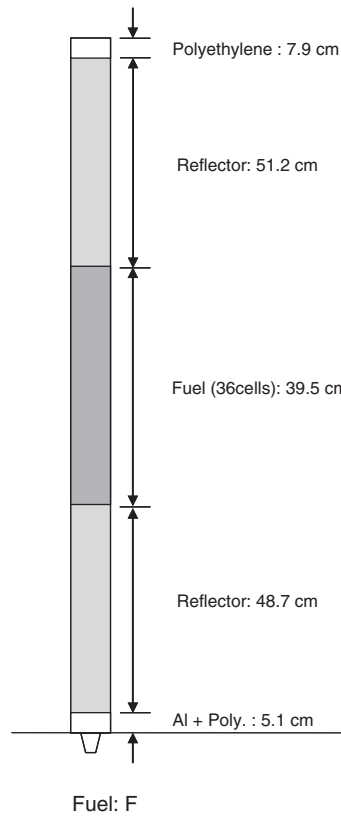


Fig. 4 Continued

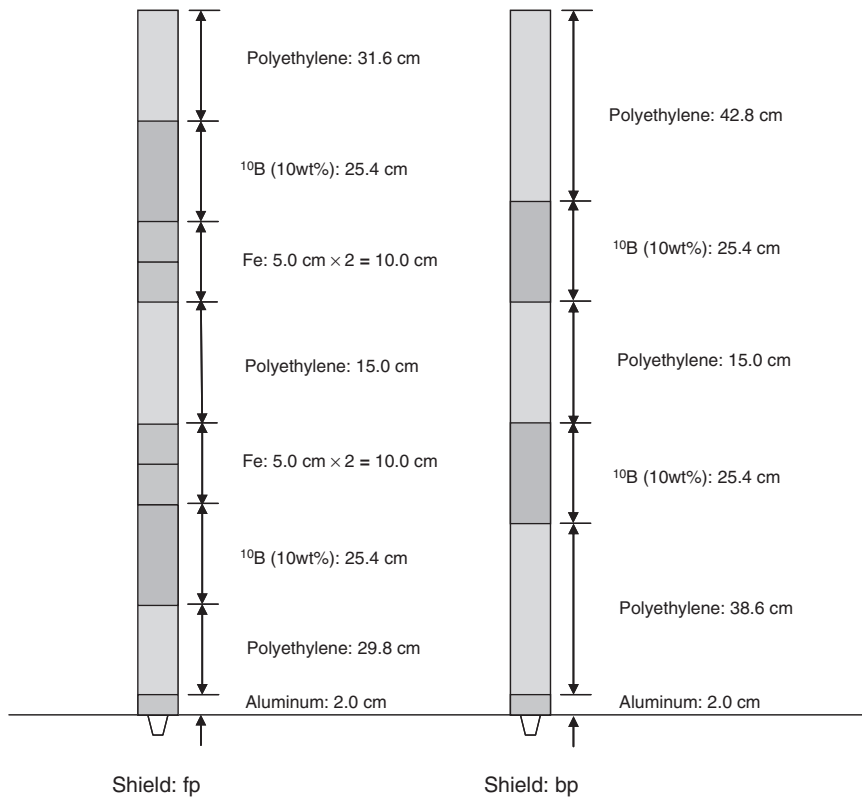
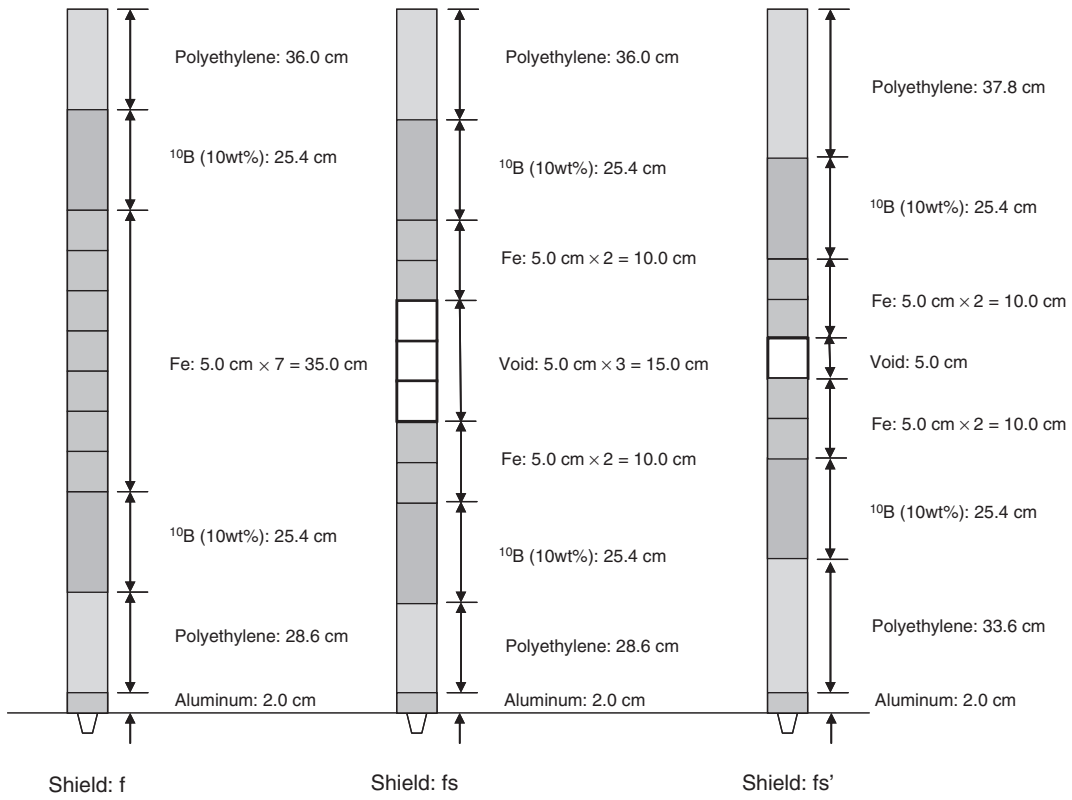


Fig. 4 *Continued*

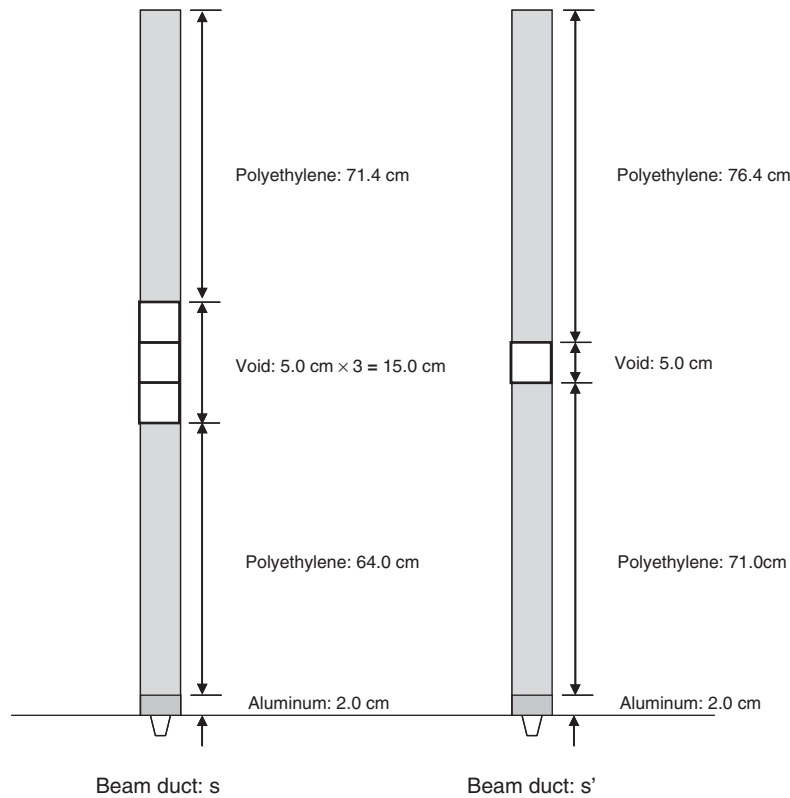


Fig. 4 Side view of fuel, neutron shield and beam duct installed in ADSR experiments with 14 MeV neutrons

about $30 \times 30 \times 40 \text{ cm}^3$. In the experiments, therefore, the neutron shield and the beam duct were installed in the polyethylene reflector region, as shown in **Fig. 3** (Neutron shield core with small beam duct: Case 2). The main purpose of installing the neutron shield and the beam duct was to direct the highest number possible of the high-energy neutrons generated in the target region to the center of the core. Also, the heavy metal target will not be placed at the center of the core due to the same reason as that for the new tritium target, even after the attachment of the FFAG accelerator. Note that the same core will be utilized in both the ADSR experiments with 150 MeV protons and those with 14 MeV neutrons.

For shielding the high-energy neutrons around the target region and thermal neutrons moderated in the reflector region, the neutron shield comprises several materials inserted into the core, as shown in **Fig. 4**: the iron (Fe) for shielding the high-energy neutrons generated in the target region by inelastic scattering reactions; the polyethylene containing 10 wt% boron (polyethylene + boron (10 wt%)) for shielding the thermal neutrons moderated by absorption reactions in the reflector region; the beam duct for directing collimated high-energy neutrons, by the streaming effect, to the core region. The cores installing the neutron shield with and without the beam duct are shown in **Figs. 5** and **6** (Neutron shield cores with large beam duct and without beam duct: Cases 3 and 4, respectively). The cores in Cases 3 and 4 were introduced into KUCA, in order to examine the window size of the beam duct in front of the fuel region and the effect of the beam duct itself on neutron multiplication by substituting the polyethylene for the beam duct, respectively.

3. Measurements

The experiments were carried out in the subcritical state by using the pulsed neutron generator. The reaction rate distribution and the neutron spectrum were then measured by the foil activation method. The critical state was adjusted by maintaining the control rods in certain positions, and the subcritical state was acquired by inserting the control or safety rods, or both, up to the lower limit in the critical state. The subcriticality was obtained from the combination of both the reactivity worth of each control rod evaluated by the rod drop method and its integral calibration curve obtained by the positive period method. The experimental error of reactivity measurement was estimated to be less than 10%. Indium (In) wire 1.5 mm ϕ in diameter and 60 cm long was set in the axial center position of (16,17–J,W) along the vertical shown in Figs. 1, 3, 5 and 6, for measuring the reaction rate distribution; and activation foils were set both in front of the target and the fuel region for measuring the neutron spectrum. (16,17–J,W) indicates the vertical line from “J” to “W” between the horizontal positions “16” and “17” shown in Figs. 1, 3, 5 and 6. The size of the activation foils was 50 mm \times 50 mm with thickness varying between 3 and 5 mm. They were selected for covering as wide a range as possible of threshold energy values within 14 MeV. The experimental results of the reaction rates of all the irradiated components, including the In wire and the activation foils, were obtained by measuring total counts of the peak energy of γ -ray emittance and normalized by the counts of another irradiated In foil ($20 \times 20 \times 1 \text{ mm}^3$) undergoing $^{115}\text{In}(n,n')^{115\text{m}}\text{In}$ reactions set in the location of the tritium target.

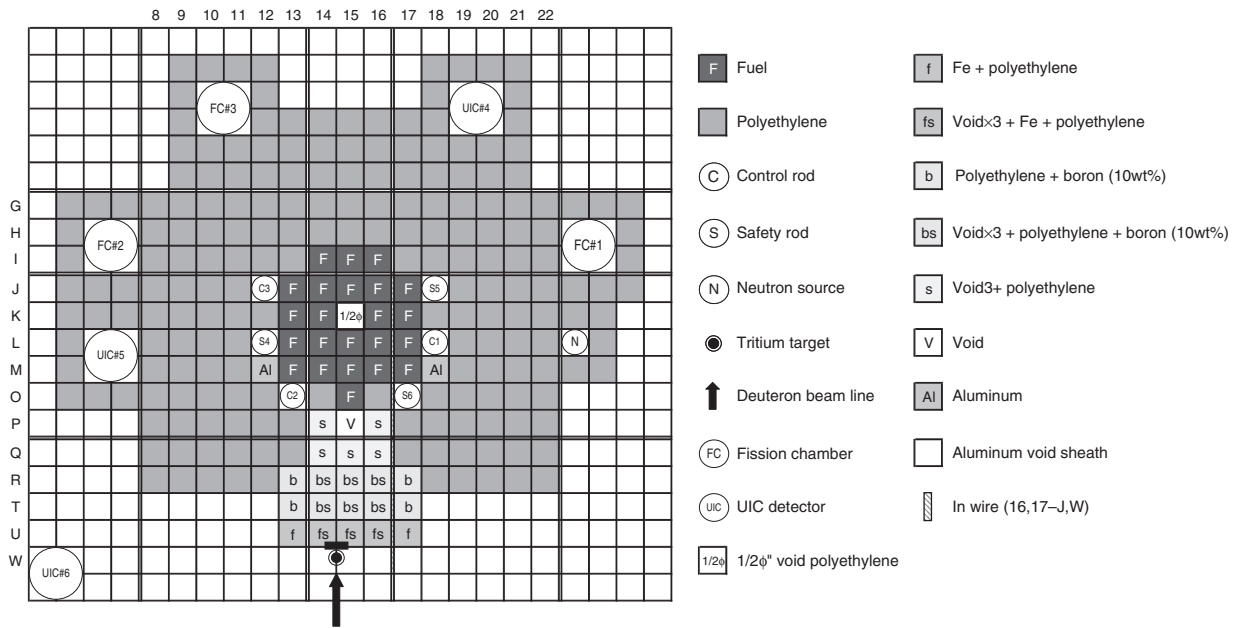


Fig. 5 Top view of configuration of A-core experiments (Neutron shield core with large beam duct: Case 3)

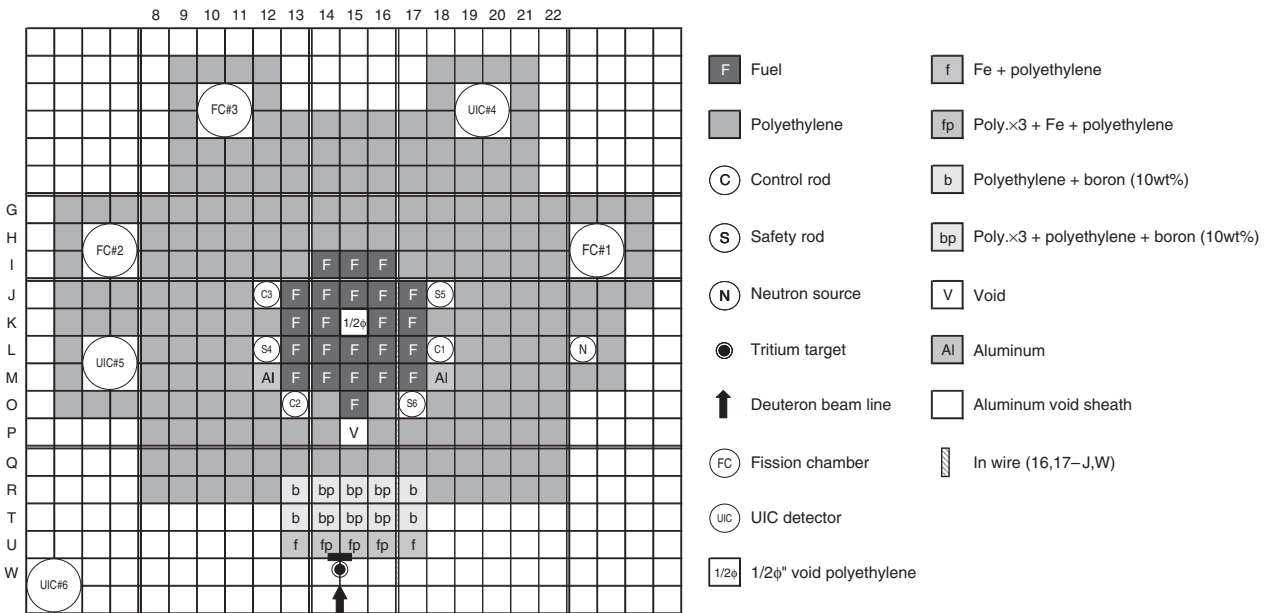


Fig. 6 Top view of configuration of A-core experiments (Neutron shield core without beam duct: Case 4)

III. Results and Discussion

The numerical analyses of the experiments described in Sec. II were executed with the use of the Monte Carlo calculation code MCNP-4C3 with the ENDF/B-VI.2 nuclear data library. The eigenvalue calculations were executed to obtain the subcriticality in the subcritical state and the excess reactivity in the critical state, while the fixed-source calculations were conducted to obtain the values of the reaction rates yielded by the In wire and the activation foils assuming continuous injection of 14 MeV neutrons into the subcritical assembly. The analyses of the neutron spectrum were carried out using an unfolding code SAND-II²⁵⁾ together with MCNP-4C3 and JENDL Activation Cross Section File 96

for the initial guess results of threshold reaction rates. Note that the MCNP statistical error was one standard deviation of 0.03% $\Delta k/k$ in multiplication factor k_{eff} and the number of neutron histories was 2×10^7 .

1. Reactivity

A comparison between the measured and calculated subcriticalities showed that for each core the calculated subcriticality $\rho_{cal-sub}$ was in good agreement with the measured $\rho_{exp-sub}$ within the relative difference of 5% shown in Table 2. On the other hand, excess reactivity was analyzed within allowances for experimental error and MCNP statistical error, although these small-reactivity analyses revealed the discrepancy between the measured $\rho_{exp-exc}$ and calculated

Table 2 Comparison between measured and calculated subcriticalities obtained from ADSR experiments and MCNP-4C3 calculations with ENDF/B-VI.2

Case	Measurement $\rho_{exp-sub}$ (% $\Delta k/k$)	Calculation $\rho_{cal-sub}$ (% $\Delta k/k$)	Relative difference (%)
1	0.90 ± 0.05	0.91 ± 0.03	1.1
2	0.93 ± 0.05	0.89 ± 0.03	4.3
3	1.17 ± 0.06	1.12 ± 0.03	4.3
4	0.91 ± 0.05	0.89 ± 0.03	2.2

Table 3 Comparison between measured and calculated excess reactivities obtained from ADSR experiments and MCNP-4C3 calculations with ENDF/B-VI.2

Case	Measurement $\rho_{exp-excess}$ (% $\Delta k/k$)	Calculation $\rho_{cal-excess}$ (% $\Delta k/k$)	Relative difference (%)
1	0.30 ± 0.02	0.33 ± 0.03	10.0
2	0.29 ± 0.02	0.33 ± 0.03	13.8
3	0.02 ± 0.01	0.06 ± 0.03	Too large
4	0.30 ± 0.02	0.32 ± 0.03	6.7

$\rho_{cal-exc}$ values, in the relative difference of over 10%, as shown in **Table 3**. These results demonstrate that exact eigenvalue calculation studies relevant to the reactivity analyses of the ADSR with 14 MeV neutrons loaded with highly enriched uranium fuel are feasible with the combined use of MCNP-4C3 and ENDF/B-VI.2, except for the small-reactivity analyses.

2. Reaction Rate Distribution

The experimental results of the reaction rate distribution obtained by $^{115}\text{In}(n, \gamma)^{116\text{m}}\text{In}$ reactions are given for the subcriticalities of about 0.9 to 1.2% $\Delta k/k$, as shown in **Fig. 7**. The reaction rates of Case 3 decreased to a greater extent than those of Case 1 in the neutron shield (reflector) region; inversely, these increased about two times in the fuel region. These results showed that the effects of the combination of the neutron shield and the beam duct were clearly exerted in both the neutron shield and the fuel regions. In other words, the experiments demonstrated that the high-energy neutrons were shielded by Fe around the target region, the moderated thermal neutrons were shielded by polyethylene with 10 wt% boron in front of the fuel region, and the high-energy neutrons flowed through the beam duct. Moreover, from the results of the reaction rates in Cases 2 and 3, it was considered that the window size of the beam duct in Case 3 was more effective in front of the fuel region than in Case 2. The results of Cases 3 and 4 showed the effect of the beam duct itself, since it is possible to compare the difference between the beam duct and the polyethylene in the neutron shield region. Therefore, an optimized combination of the neutron shield and the size of the beam duct was made to efficiently direct the high-energy neutrons to the fuel region. Thus, the installation of the neutron shield and the beam duct was valid for directing the high-energy neutrons to the fuel region, and the pattern of the neutron shield

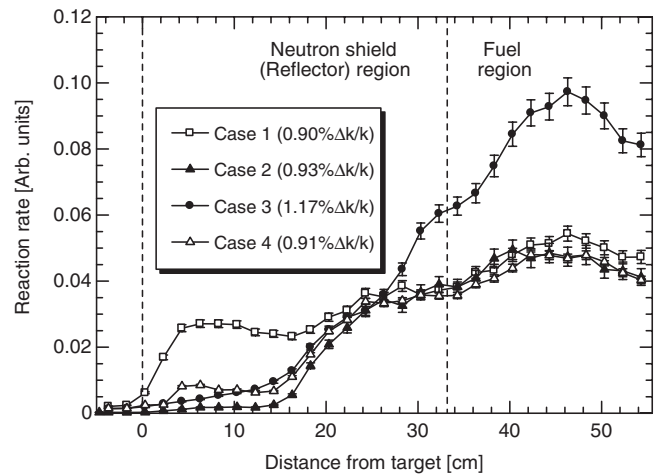


Fig. 7 Measured reaction rate distributions in Cases 1 through 4 using In wire along vertical of (16, 17-J, W) shown in Figs. 1, 3, 5 and 6

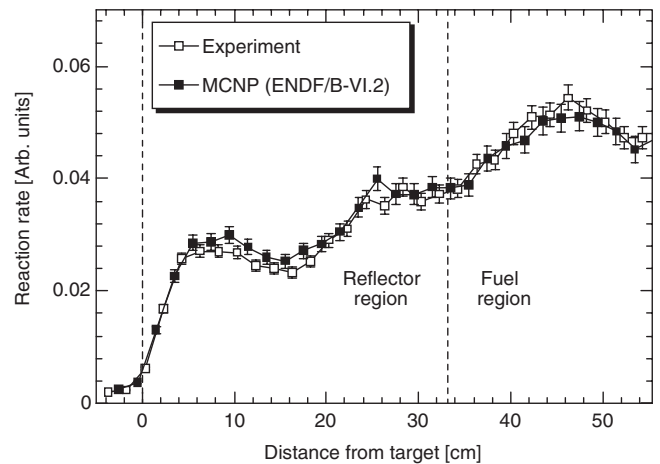


Fig. 8 Comparison between measured and calculated reaction rate distributions in Case 1 using In wire along vertical of (16, 17-J, W) shown in Fig. 1

and the beam duct shown in Case 3 was experimentally appropriate for the purpose of the installation of the neutron shield and the beam duct, as demonstrated by the comparison between the results of the reaction rate distributions.

A comparison between the measured and calculated reaction rate distributions for the cores used in Cases 1 and 3 demonstrated that the configuration of the measured reaction rate distribution obtained approximately by the fixed-source calculation based on the combined use of MCNP-4C3 and ENDF/B-VI.2 shown in **Figs. 8** and **9**, respectively, is valid.

3. Neutron Spectrum

In measuring the neutron spectrum, the activation foils were set as an aggregate of several samples in the region of interest, in front of the fuel region, for obtaining neutron spectral information on how much the high-energy neutrons generated in the target could be directed to the fuel region, in terms of the reaction rates. At KUCA, this measuring technique is used for irradiating all the foils at once and is called

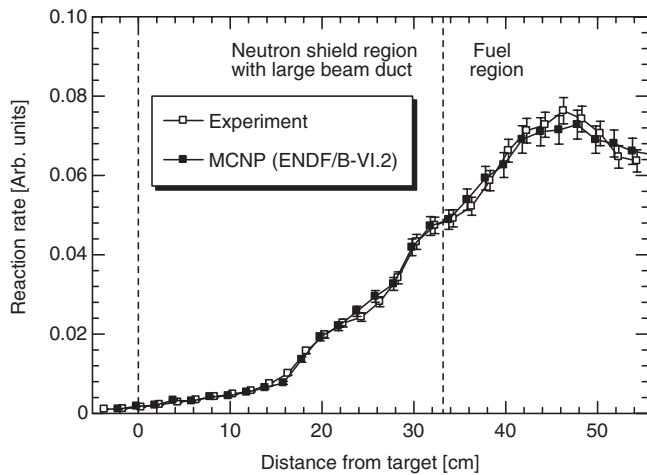


Fig. 9 Comparison between measured and calculated reaction rate distributions in Case 3 using In wire along vertical of (16, 17-J, W) shown in Fig. 5

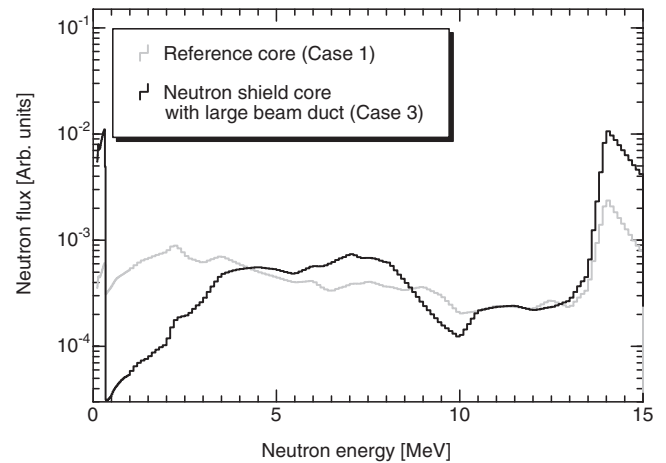


Fig. 10 Comparison between measured neutron spectrums in Cases 1 and 3 using SAND-II at position (15, P) shown in Fig. 1

Table 4 Measured reaction rates of irradiated foils normalized by another In foil attached to the target in Cases 1 and 3

Reaction	Threshold (MeV)	Irradiation position			
		Target (Case 1)	Target (Case 3)	(15, P) (Case 1)	(15, P) (Case 3)
$^{115}\text{In} (n, n') ^{115\text{m}}\text{In}$	0.32	1.00 ± 0.15	1.00 ± 0.19	0.96 ± 0.14	1.68 ± 0.29
$^{60}\text{Ni} (n, p) ^{60}\text{Co}$	2.08	5.31 ± 1.23	5.05 ± 0.35	0.73 ± 0.40	4.21 ± 2.51
$^{56}\text{Fe} (n, p) ^{56}\text{Mn}$	2.97	3.40 ± 0.28	3.66 ± 0.38	1.27 ± 0.11	2.51 ± 0.41
$^{27}\text{Al} (n, \alpha) ^{24}\text{Na}$	3.25	2.26 ± 0.36	2.58 ± 0.11	0.29 ± 0.02	0.69 ± 0.10
$^{24}\text{Mg} (n, p) ^{24}\text{Na}$	4.93	0.51 ± 0.07	0.51 ± 0.08	0.14 ± 0.01	0.25 ± 0.03
$^{127}\text{I} (n, 2n) ^{126}\text{I}$	9.22	4.37 ± 0.18	5.25 ± 0.68	0.43 ± 0.08	1.59 ± 0.21
$^{58}\text{Ni} (n, 2n) ^{57}\text{Ni}$	12.43	0.30 ± 0.31	0.31 ± 0.38	—	—

the multifoil activation method. The activation foils were selected for covering a wide range of threshold energy values, and are 50 mm \times 50 mm in area and 3 to 5 mm thick. The ^{24}Mg and ^{127}I samples were in powder forms of MgO and NaI, respectively. The results of the reaction rates were normalized by that of the In foil emitted from $^{115}\text{In} (n, n') ^{115\text{m}}\text{In}$ reactions at the attached target. The results of measured reaction rates were obtained from those of saturated radioactivity on the basis of the γ -ray emission counts by using the high-purity germanium (HPGe) detector. The experimental errors in the activation foils were estimated to be 10 to 15% including the detection efficiency and the statistical errors of γ -ray counts.

The experimental results were relatively larger by about two to four times with the neutron shield and the beam duct than without them at position (15, P) corresponding to the position in front of the fuel region, shown in Table 4, while insufficient activation by irradiating neutrons caused a noticeable error by a few counts of γ -ray emittance in the experimental results of ^{58}Ni and ^{60}Ni . Apparently, the effects of the neutron shield and the beam duct were also observed in the reaction rates at position (15, P) of other irradiated activation foils by the multifoil activation method, comparing the results of Case 3 with those of Case 1.

The results of the neutron spectrum at position (15, P)

evaluated using SAND-II demonstrated that the neutron flux of high-energy neutrons in the range of 14 MeV at position (15, P) was obtained to be relatively larger in Case 3 than in Case 1 about two times as shown in Fig. 10; and the effects of the neutron shield and the beam duct were revealed in the neutron flux over two times at 14 MeV through the neutron spectrum analyses. In other words, it was considered that the difference between the cores with and without the neutron shield and the beam duct was also confirmed by the unfolding analyses. As shown in Fig. 11, the comparison between the results of the experiments using SAND-II and the calculations using MCNP-4C3 showed that the precision of the unfolding analyses was not enough to evaluate exactly the neutron spectrum, from the viewpoint of establishing the measurement techniques.

IV. Conclusions

A series of preliminary experiments on the ADSR with 14 MeV neutrons were carried out at KUCA by the foil activation method, prior to the ADSR experiments with 150 MeV protons. The experiments and analyses using MCNP-4C3 revealed the following:

1. With the combined use of MCNP-4C3 and ENDF/B-VI.2, we can carry out precise eigenvalue calculations

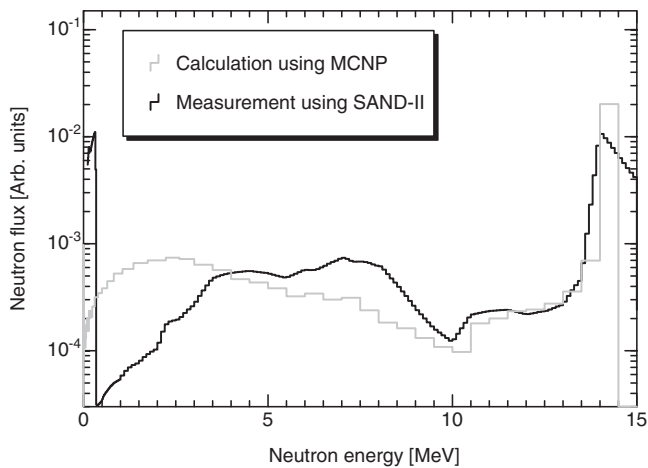


Fig. 11 Comparison between measured and calculated neutron spectrums in Case 3 at position (15, P) shown in Fig. 1

relevant to the reactivity analyses of the ADSR with 14 MeV neutrons within the relative difference of about 5%, as well as to the subcriticality in the subcritical system, except for the small-reactivity analyses. The configuration of the measured reaction rate distribution in the subcritical system can be reconstructed well by fixed-source calculations based on the combined use of MCNP-4C3 and ENDF/B-VI.2.

2. The effects of the neutron shield and the beam duct can be validly confirmed through the measurements of both reaction rate distribution using In wire and reaction rates using irradiated activation foils. Also, these effects can be experimentally evaluated through unfolding analyses obtained using SAND-II with MCNP-4C3 and JENDL Activation Cross Section File 96.
3. The foil activation method was found to be a useful measurement technique for examining the neutronic properties of the ADSR with 14 MeV neutrons at KUCA through these preliminary experiments.

Further studies are needed to examine experimental values against representative subcriticality levels (around $k_{eff} = 0.95$) of an actual ADSR and to update optimization of the beam duct, especially in the fuel region. Numerically, another method is requisite in the evaluation of neutron spectrum properties, such as C/E evaluation of the difference between measured and calculated reaction rates, and in examining the difference in nuclear data libraries between JENDL Activation Cross Section File 96 and others. Both the foil activation method and numerical Monte Carlo simulations could also be applied in the further analyses of not only 14 MeV neutrons generated by D-T reactions but the high-energy neutrons generated by 150 MeV protons in the FFAG accelerator, since the ADSR experiments with 150 MeV protons will be carried out at the same core as those with 14 MeV neutrons.

Acknowledgements

The authors extend special thanks to all KUCA staff members for carrying out these experiments and to Mr. Morgan

Helvult of Kyoto University for his contribution in executing the computational procedures.

References

- 1) R. Soule, W. Assal, P. Chaussonnet, *et al.*, "Neutronic studies in support of accelerator-driven systems: The MUSE experiments in the MASURCA facility," *Nucl. Sci. Eng.*, **148**, 124 (2004).
- 2) T. Sasa, H. Oigawa, K. Tsujimoto, K. Nishihara, *et al.*, "Research and development on accelerator-driven transmutation system at JAERI," *Nucl. Eng. Design*, **230**, 209 (2004).
- 3) K. Tsujimoto, T. Sasa, K. Nishihara, H. Oigawa, H. Takano, "Neutronics design for lead-bismuth cooled accelerator-driven system for transmutation of minor actinide," *J. Nucl. Sci. Technol.*, **41**, 21 (2004).
- 4) M. Eriksson, J. E. Cahalan, W. S. Yang, "On the performance of point kinetics for the analysis of accelerator-driven systems," *Nucl. Sci. Eng.*, **149**, 298 (2005).
- 5) C. Jammes, B. Geslot, R. Rosa, G. Imel, P. Fougeras, "Comparison of reactivity estimations obtained from rod-drop and pulsed neutron source experiments," *Ann. Nucl. Energy*, **32**, 1131 (2005).
- 6) A. Rineiski, W. Maschek, "Kinetics models for safety studies of accelerator driven systems," *Ann. Nucl. Energy*, **32**, 1348 (2005).
- 7) M. Mori, S. Shiroya, K. Kanda, "Temperature coefficient of reactivity in light-water moderated and reflected cores loaded with highly-enriched-uranium fuel," *J. Nucl. Sci. Technol.*, **24**, 653 (1987).
- 8) S. Shiroya, K. Kanda, K. Tsuchihashi, "Analyses of reactor physics experiments in the Kyoto University Critical Assembly," *Nucl. Sci. Eng.*, **100**, 525 (1988).
- 9) T. Misawa, S. Shiroya, K. Kanda, "Study on criticality of a light water moderated and reflected coupled core with highly enriched uranium fuel," *Nucl. Technol.*, **83**, 162 (1988).
- 10) T. Misawa, S. Shiroya, K. Kanda, "Measurement of prompt neutron decay constant and large subcriticality by the Feynman- α method," *Nucl. Sci. Eng.*, **104**, 53 (1990).
- 11) N. Hirakawa, H. Nara, T. Iwasaki, K. Kobayashi, K. Kudo, "Measurement and analysis of cadmium ratios of activation foils in thermal critical assembly (KUCA B 3/8" P36EU-NU-EU)," *J. Nucl. Sci. Technol.*, **30**, 628 (1993).
- 12) Y. Yamane, Y. Hirano, S. Shiroya, K. Kobayashi, "Measurement of reactivity effect and thermal neutron flux in non-uniformity distributed fuel assemblies," *J. Nucl. Sci. Technol.*, **31**, 640 (1994).
- 13) K. Hashimoto, T. Sano, H. Unesaki, T. Kitada, J. Yamamoto, T. Horiguchi, T. Takeda, O. Aizawa, S. Shiroya, "Rapid estimation of core-power ratio in coupled-core system by rod drop method," *J. Nucl. Sci. Technol.*, **37**, 565 (2000).
- 14) H. Unesaki, T. Iwasaki, T. Kitada, A. Kohashi, D. Fujiwara, M. Kuroda, T. Kato, Y. Ikeuchi, S. Shiroya, "Measurement of ^{237}Np fission rate ratio relative to ^{235}U fission rate on cores with various thermal neutrons spectrum at the Kyoto University Critical Assembly," *J. Nucl. Sci. Technol.*, **37**, 625 (2000).
- 15) T. Iwasaki, T. Horiuchi, D. Fujiwara, H. Unesaki, S. Shiroya, M. Hayashi, H. Nakamura, T. Kitada, N. Shinohara, "Measurement and analyses of capture reactions rate of ^{237}Np in various thermal neutron fields by critical assembly and heavy water thermal neutron facility of Kyoto University," *Nucl. Sci. Eng.*, **136**, 321 (2000).
- 16) S. Shiroya, H. Unesaki, Y. Kawase, H. Moriyama, M. Inoue, "Accelerator driven subcritical system as a future neutron

- source in Kyoto University Research Reactor Institute (KURRI)—Basic study on neutron multiplication in the accelerator driven subcritical reactor,” *Prog. Nucl. Energy*, **37**, 357 (2000).
- 17) S. Shiroya, A. Yamamoto, K. Shin, T. Ikeda, S. Nakano, H. Unesaki, “Basic study on accelerator driven subcritical reactor in Kyoto University Research Reactor Institute (KURRI),” *Prog. Nucl. Energy*, **40**, 489 (2002).
 - 18) S. Machida, “Neutrino factory design based on FFAG,” *Nucl. Instrum. Methods A*, **503**, 41 (2003).
 - 19) S. Machida, “Design and particle tracking of FFAG,” *Nucl. Instrum. Methods A*, **503**, 318 (2003).
 - 20) Y. Mori, “FFAG proton driver for muon source,” *Nucl. Instrum. Methods A*, **451**, 300 (2000).
 - 21) C. Ichihara, *et al.*, “Characteristics of KUCA pulsed neutron generator,” *Kyoto University Research Reactor Institute Technical Report*, KURRI-TR-240, (1983) [in Japanese].
 - 22) J. F. Briesmeister, Editor, “MCNP-A general Monte Carlo N-particle transport code, Version 4C,” *LANL Report LA-13709-M*, Los Alamos National Laboratory, (2000).
 - 23) P. F. Rose, “ENDF-201, ENDF/B-VI Summary Documentation,” BNL-NCS-17541, 4th Edition (1991).
 - 24) Y. Nakajima, “JNDC WG on activation cross section data: JENDL activation cross section file,” *Proc. 1990 Symposium on Nuclear Data*, JAERI-M 91-032, 43 (1991).
 - 25) W. N. McEloy, S. Berg, G. Gigas, “Neutron-flux spectral determination by foil activation,” *Nucl. Sci. Eng.*, **27**, 533 (1967).
-